HHS Public Access

Author manuscript

Exp Eye Res. Author manuscript; available in PMC 2018 July 01.

Published in final edited form as:

Exp Eye Res. 2017 July ; 160: 45–55. doi:10.1016/j.exer.2017.04.010.

Quercetin and cyanidin-3-glucoside protect against photooxidation and photodegradation of A2E in retinal pigment epithelial cells

Yong Wang[a], **Hye Jin Kim**[a], and **Janet R. Sparrow**[a,b,*]

[a]Department of Ophthalmology, Columbia University Medical Center, New York, NY 10032

[b]Department of Pathology and Cell Biology, Columbia University Medical Center, New York, NY 10032

Abstract

A family of photoreactive retinaldehyde-derived molecules accumulate in retinal pigment epithelial cells with age; this accumulation is implicated in some retinal diseases. One of these compounds is the diretinal fluorophore A2E. Here we compared polyphenols for their ability to suppress the photooxidation and photodegradation of A2E. In cells that had accumulated A2E and were irradiated with short-wavelength light, quercetin, cyanidin-3-glucoside, ferulic acid and chlorogenic acid diminished cellular levels of reactive oxygen species, but only quercetin and cyanidin-3-glucoside promoted cell viability. By chromatographic quantitation, quercetin and cyanidin-3-glucoside reduced the consumption of A2E by photooxidation in both cell- and cell-free assays. With ultra-high performance liquid chromatography-mass spectrometry, quercetin and cyanidin-3-glucoside also inhibited the formation of photooxidized-A2E species. While photodegradation of A2E is known to result in the release of reactive carbonyls, we demonstrated that quercetin and cyanidin-3-glucoside decreased the formation of methylglyoxal adducts in the cells, and reduced the expression of mRNA encoding receptor for advanced glycation end products. These polyphenols also protected glutathione from reaction with photooxidized A2E. In rod outer segments incubated with all-*trans*-retinal to generate bisretinoid, followed by irradiation, quercetin and cyanidin-3-glucoside reduced release of the lipid peroxidation product 4-hydroxynonenal. In conclusion, quercetin and cyanidin-3-glucoside can guard against photooxidative processes in retina.

Graphical Abstract

*Corresponding author: jrs88@cumc.columbia.edu (Janet R. Sparrow).

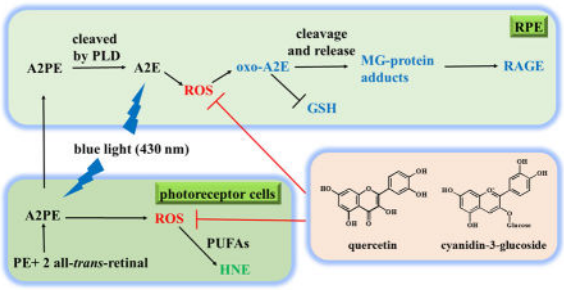

Keywords

bisretinoid; A2E; photooxidation; photodegradation; methylglyoxal; receptor for advanced glycation end products (RAGE)

1. Introduction

Fluorophores having bisretinoid structures are produced in the membranes of photoreceptor outer segments (OSs) due to inadvertent non-enzymatic reactions of vitamin A-aldehyde. These compounds are subsequently transferred to retinal pigment epithelial (RPE) cells within phagocytosed OS disks and accumulate in RPE as lipofuscin (Sparrow et al., 2003a). A2E, just one of a complex mixture of bisretinoids that are accrued in this way, exhibits detergent-like activity and has photo-sensitive properties that can be a source of oxidative stress in RPE (Liu et al., 2000; Mata et al., 2000).

For all of the bisretinoids of RPE lipofuscin, the two-armed polyene structures terminating in β-ionone rings confer the extended conjugation systems that enable the short arm of the molecule to absorb in the UV range and the long arm to absorb in the visible region of the spectrum (Sparrow et al., 2010). For instance, A2E has an absorbance maximum in the visible spectrum at ~440 nm and a shorter wavelength absorbance at ~340 nm. Absorbances in the visible portion of the spectrum are significant because they reach the retina (Sparrow et al., 2012).

Upon irradiation with short-wavelength visible light, A2E acts as a photosensitizer generating singlet oxygen and other reactive oxygen species (ROS) (Ben-Shabat et al., 2002; Kim et al., 2008). A2E is also an excellent quencher of singlet oxygen. Consequently, singlet oxygen subsequently adds to carbon–carbon double bonds of bisretinoid molecules (photooxidation) thereby forming endoperoxides, epoxides, and furanoid moieties that have been identified in hydrophobic extracts of human and mouse retina (Ben-Shabat et al., 2002; Jang et al., 2005a). At these oxidation sites bisretinoids undergo cleavage, releasing aldehyde- and carbonyl bearing molecular fragments such as the dicarbonyls methylglyoxal (MG) and glyoxal. These dicarbonyls can react with and inactivate proteins (Wu et al., 2010). They can also provoke the formation of advanced glycation end products (AGE) that deposit extracellularly (Yoon et al., 2012; Zhou et al., 2005) and incite the upregulation of the receptor for advanced glycation end product (RAGE) (Zhou et al., 2015). Because these AGE-modified proteins are present in deposits (drusen) that accumulate on the basal side of

RPE cells *in vivo*, and drusen are a major risk factor for AMD pathogenesis, the photodegradation of bisretinoids may constitute a molecular link to drusen and AMD (Anderson et al., 2002; Crabb et al., 2002).

We have previously demonstrated a role for antioxidants such as bilberry-derived anthocyanins and vitamin E, in protecting against bisretinoid photoxidation by scavenging singlet oxygen (Sparrow et al., 2003b). Quercetin, cyanidin-3-glucoside, protocatechuic acid, ferulic acid, and chlorogenic acid are common plant polyphenols known to have protective effects on retinal light damage *in vitro* and *in vivo* (Saviranta et al., 2011; Tremblay et al., 2013; Wang et al., 2015; Wang et al., 2016; Wang et al., 2017). Cyanidin-3-glucoside and its phenolic acid metabolites (protocatechuic acid and ferulic acid) attenuated light-induced retinal oxidative stress, inflammation and apoptosis in pigmented rabbits via activation of Nrf2/HO-1 pathway and NF-κB suppression (Wang et al., 2016). Furthermore, quercetin and cyanidin-3-glucoside with *ortho* phenolic groups probably possess antioxidative properties capable of suppressing photooxidation (Wang et al., 2015; Wright et al., 2001). However, whether these common polyphenols protect against RPE damage via suppressing bisretinoid photooxidation/photodegradation has yet to be elucidated.

In this study, we investigated the effects of five common polyphenols on blue light irradiated A2E-containing RPE cells. Polyphenols, the most abundant phytochemicals in fruits and vegetables, can be divided into several classes according to their carbon backbone. These classes include phenolic acids (hydroxybenzoic acids, C6–C1; hydroxycinnamic acids, C6–C3), flavonoids (C6–C3–C6), stilbenes (C6-C2-C6), lignans (C6–C3–C3–C6) and others (Milenkovic et al., 2013). Flavonoids include 6 subclasses: anthocyanins, flavanols, flavonols, flavones, flavanones, and isoflavones. Of the five polyphenols investigated in this study, protocatechuic acid, ferulic acid and chlorogenic acid belong to the class of phenolic acids. Quercetin and cyanidin-3-glucoside are flavonoids. In addition to quantifying cell viability, we measured ROS levels and pathways reflecting the downstream effects of bisretinoid photodegradation. This is the first report of the protective effects of quercetin and cyanidin-3-glucoside on inhibiting the photooxidation and photodegradation of A2E in RPE cells and in cell-free assays.

2. Materials and Methods

2.1. Synthesis of A2E

A2E was synthesized by incubating all-*trans*-retinal (atRAL) with ethanolamine as published (Parish et al., 1998); purification was by HPLC.

2.2. Cell culture and illumination

Human adult RPE cells (ARPE-19, American Type Culture Collection, Manassas, VA) deficient in endogenous lipofuscin (Sparrow et al., 1999) were grown to confluence as described previously (Sparrow et al., 2002). To introduce synthesized A2E to confluent cultures for accumulation in the lysosomal compartment of the cells, A2E was placed in the culture medium (3 μM final concentration with 0.01% DMSO), incubated with the cells and refreshed once every two days. The accumulation proceeded for 8 days. The cells were then

treated with and without quercetin, cyanidin-3-glucoside, protocatechuic acid, ferulic acid, or chlorogenic acid (10, 25, and 50 μM) for 24 hours prior to being exposed to 430 nm irradiation (1.5 milliwatts/cm^2, 20 or 30 min) to photooxidize A2E (Yoon et al., 2011). Incubation of the cells was continued for an additional 18 h.

2.3. Cell viability assay

Cytotoxicity was measured by 3-(4, 5-dimethylthiazol-2-yl)-2, 5-diphenyltetrazolium bromide (MTT) assay (Roche Diagnostics, Mannheim, Germany). After A2E accumulation, the cells were treated with quercetin, cyanidin-3-glucoside, protocatechuic acid, ferulic acid, and chlorogenic acid (10, 25 and 50 μM) for 24 hours in 96-well plates. The cells were exposed to 430 nm irradiation for 30 min then were incubated for 18 h at 37°C. The MTT labeling reagent was added (10 μL per well) for 4 hours after the cells were solubilized (100 μL per well) and incubated at 37°C overnight. The absorbance was read by a SpectraMax 5 microplate reader (Molecular Device Inc. Sunnyvale, CA) at 570 nm.

2.4. Measurement of cellular reactive oxygen species (ROS)

ROS were quantified in ARPE-19 cells using the fluorescent dye 2′,7′-dichlorofluorescin diacetate (DCFH-DA). To this end, ARPE-19 cells (density of 5×10^5 cells/mL) were cultured in 200 μL of growth medium and placed in 96-well black plates with transparent bottoms. After the cells had accumulated A2E as described above, the media in the treatment groups was replaced by Dulbecco's Modified Eagle Medium (DMEM) (Invitrogen, Carlsbad, CA) that contains 10 and 25 μM polyphenols (quercetin, cyanidin-3-glucoside, protocatechuic acid, ferulic acid, or chlorogenic acid) for 24 h. The ARPE-19 cells were then irradiated (430 ± 30 nm, 1.5 milliwatts/cm^2) for 30 min. Subsequently, the medium was replaced by serum-free DMEM medium that contains 25 μM DCFH-DA. The cells were incubated for another 45 min at 37°C. After the supernatant had been removed, the cells were carefully washed twice with HBSS. The fluorescence of the cells in each well was recorded by using the SpectraMax 5 microplate reader with 485 nm excitation and 530 nm emission.

2.5. Quantitative HPLC analysis of A2E photooxidation in a cell-free assay

To test the effect of polyphenols on A2E photooxidation, A2E stock (18 mM in DMSO) was diluted with DPBS (Life Technologies, Inc.) to a final concentration of 100 μM. Polyphenols were added to obtain concentrations of 100 or 200 μM and then were irradiated (430 ± 30 nm, 1.5 milliwatts/cm^2; 1 or 3 min). After vortex-mixing, samples were directly injected into an Alliance HPLC system (Waters Corp, Milford, MA) equipped with 2695 Separation Module, 2996 Photodiode Array Detector and Empower software for HPLC analysis and quantitation. Separation was carried out with an Atlantis dC18 column (3 μm, 4.6 × 150 mm; Waters Corp, Milford, MA), a gradient of acetonitrile and water containing 0.1% trifluoroacetic acid (0–30 min, 75–90% acetonitrile in water; 30–40 min, 90–100% acetonitrile in water; 40–60 min, 100% acetonitrile; flow rate, 0.5 mL/min, injection volume, 30 μL and 430 nm monitoring). Quantitation of A2E was performed using a calibration curve constructed from synthetic A2E standards.

2.6. Quantitative UPLC analysis of A2E photooxidation in a cellular assay

ARPE-19 cells that had accumulated A2E as described above treated with and without quercetin and cyanidin-3-glucoside (10 and 50 μM) for 24 hours and were exposed to 430 nm light for 20 min. The cells were then detached from the culture dish with trypsin, pelleted, washed, and counted (Bright Light Counting Chamber, Hausser Scientific Company, Horsham, PA). The harvested RPE cells were subsequently dried under argon gas and then dissolved in methanol. Samples were analyzed by UPLC with an XBridge BEH C18 column (2.5 μm, 3.0 × 50 mm; Waters Corp, Milford, MA), acetonitrile-methanol mixtures (1:1) and a water gradient with 0.1% formic acid (0–30 min, 70–98% the acetonitrile-methanol mixture in water; flow rate, 0.5 mL/min, injection volume, 5 μL and 430 nm monitoring). The quantity of A2E in each sample was calculated using a calibration curve constructed from synthetic A2E standards.

2.7. Ultra performance liquid chromatography-mass spectrometry (UPLC-MS) analysis of A2E-epoxide formation in a cell-free assay

A2E (18 mM in DMSO) was diluted in DPBS to a final A2E concentration of 100 μM. Quercetin and cyanidin-3-glucoside were then added to obtain concentrations of 100 and 200 μM, and were irradiated (430 ± 30 nm, 1.5 milliwatts/cm^2) for 3 min. The samples were examined by UPLC with a Waters SQ Detector (ion source; electrospray ionization mode (ESI), mass analyzer; single quadrupole). To acquire full scans, 5 μL of each sample was directly injected (without column) with a solvent of 70% acetonitrile/methanol (1:1) in 30% water containing 0.1% formic acid at a flow rate of 0.5 mL/min. UPLC-MS analysis was performed using positive ionization mode and voltages as follows: capillary voltage, 3.0 V; cone voltage, 30 V; extractor voltage, 3 V; and radio frequence lens voltage, 0.1 V. The desolvation gas flow was 800 liters/hr and the cone gas flow was 50 liters/hr; the source temperature was 150 °C, and desolvation temperature was 400 °C.

2.8. Colorimetric assay of glutathione (GSH)

To test for whether quercetin and cyanidin-3-glucoside inhibit the reactivity of photooxo-A2E with GSH, we measured residual GSH after reduction of 5,5′-dithiobis-(2-nitrobenzoic acid) (DTNB) to the yellow colored product 2-nitro-5-thiobenzoic acid. Accordingly, GSH (200 μM; ApoGSH Glutathione Colorimetric Detection Kit; BioVision Research Products, Mountain View, CA) in buffer containing 1% sulfosalicylic acid was prepared with and without 200 μM A2E and was combined with quercetin and cyanidin-3-glucoside (200 μM). Irradiation (430 ± 30 nm, 1.5 milliwatts/cm^2; 15 min) was performed after the samples were incubated for 6 h at 37 °C. The reaction mixture included GSH reductase and nicotinamide adenine dinucleotide phosphate oxidase (BioVision Research Products; reagents of ApoGSH kit). Subsequently, DTNB (60 μM; BioVision Research Products) was added. After 10 min, absorbance at 405 nm was read in the SpectraMax 5 microplate reader.

2.9. Detection of MG-RNase A adducts in acellular assay

A2E (18 mM in DMSO) was diluted with RNase A (10 mg/ml in DPBS; Sigma-Aldrich Corp.) to a final A2E concentration of 100 μM, quercetin and cyanidin-3-glucoside were added to obtain final concentrations of 100, 200 and 500 μM. After irradiation (430 ± 30 nm,

1.5 milliwatts/cm^2; 30 min), the mixture was incubated (5 days, 37 °C, with stirring) to generate MG-RNase A adducts. MG-RNase A adducts were quantified by competitive indirect ELISA (OxiSelect, Cell Biolabs).

2.10. Detection of MG adducts in RPE cells

MG-derived hydroimidazolone (MG-H1) protein adducts were quantified in ARPE-19 cells that had accumulated A2E for 8 days as described above and were exposed to 430 nm light for 20 min. RPE cells were placed in lysis buffer (Cell Signaling, Danvers, MA) with protease inhibitors (complete protease inhibitor mixture tablets, Roche Applied Science) on ice; and the cells were released with a scraper. After centrifuging the lysates at 14,000 rpm and 4 °C, the protein concentration of the supernatant was determined by using BCA protein assay (Pierce), and MG-H1 protein adducts were quantified by competitive indirect ELISA (OxiSelect, Cell Biolabs). Absorbance was read at 450 nm; MG content was determined by comparison with a standard curve constructed using MG-BSA.

2.11. Real time quantitative polymerase chain reaction (RT-qPCR)

Total RNA was extracted with Trizol (Invitrogen, Carlsbad, CA). Complementary DNA (cDNA) was generated by reverse transcription of isolated RNA (1μg of total RNA) using the High Capacity cDNA Reverse Transcription Kit (Applied Biosystems) according to the manufacturer's protocol. The reactions were diluted 1:5 and 2 μL cDNA product was used per 20 μL PCR reaction. Real-time PCR was performed using Power SYBR Green master mix (Applied Biosystems) protocol in a StepOne Plus system (Applied Biosystems, Foster City, CA, USA). Gene expression in each sample was normalized ($2^{-\Delta\Delta Ct}$) to β-actin expression. The primer sequences used were as follows: for RAGE, 5′-GCTGGAATGGAAACTGAACACAGG-3′ (forward) and ′5′-TTCCCAGGAATCTGGTAGACACG-3′ (reverse); for β-actin, 5′-TCCCTGGAGAAGAGCTACGA-3′ (forward) and 5′-AGCACTGTGTTGGCGTACAG-3′ (reverse). Real-time PCRs were performed in triplicate.

2.12. 4-hydroxynonenal (HNE) detection in rod OSs

Rod OSs isolated from 50 bovine eyes (InVision BioResources, Seattle, WA) were diluted in 4.8 mL DPBS; atRAL was added to yield a final concentration of 5 mM. The mixture was then incubated at 37 °C for 72 h in the dark. Unbound atRAL was removed by repeating the wash (3 times in DPBS). The OSs mixture was then incubated with quercetin and cyanidin-3-glucoside (200 and 500 μM) at 37 °C for 2 h. The samples were exposed to 430 nm light for 30 min and were solubilized by lysis buffer, HNE was then quantified by ELISA (OxiSelect, Cell Biolabs).

2.13. Statistical Analysis

Statistical analysis was carried out using GraphPad Prism, version 6 (GraphPad Software, Inc. La Jolla, CA), and $p < 0.05$ was considered significant.

3. Results

3.1. Effect of polyphenols on the viability of irradiated A2E-containing RPE cells

To examine the propensity of polyphenols to combat photooxidative mechanisms, we employed a cell culture model within which A2E is allowed to accumulate in the lysosomal compartment of ARPE-19 cells (Sparrow et al., 2002). In cells that accumulated A2E alone viability was not reduced. However, the survival was reduced to approximately 60% in A2E-containing RPE cells that were also irradiated (Fig. 1A). Of the 5 antioxidants we tested, only quercetin (50 μM) and cyanidin-3-glucoside (25 and 50 μM) significantly increased cell viability compared with the irradiated A2E-containing cell group ($p < 0.05$) (Fig. 1B–F).

3.2. Polyphenol antioxidants suppress ROS levels in RPE cells

The generation of ROS was probed using the fluorescent dye DCFH-DA; in the presence of intracellular ROS, this dye is converted to highly fluorescent dichlorofluorescein. After irradiation, the ROS level in A2E-containing RPE cells was increased 14.9-fold compared to the untreated RPE cells (Fig. 2). At a concentration of 25 μM, quercetin, cyanidin-3-glucoside, ferulic acid and chlorogenic acid markedly diminished ROS levels in irradiated A2E-containing RPE cells ($p < 0.05$). Among these antioxidants, cyanidin-3-glucoside (25 μM) exhibited the strongest ROS-scavenging activity with ROS levels being diminished by 52.2%.

3.3. Polyphenols suppress A2E photooxidation in cell-free and cellular assays

Using a cell-free assay, we compared the abilities of quercetin, cyanidin-3-glucoside, protocatechuic acid, ferulic acid and chlorogenic acid to restrain A2E photooxidation (Fig. 3A). Measured as the loss of A2E due to photooxidation, we observed that with 430 nm-irradiation of A2E for 1 min in the presence of the antioxidants (200 μM; 1:2 molar ratio, A2E to antioxidants), only quercetin and cyanidin-3-glucoside exhibited protective effects by inhibiting A2E photooxidation ($p < 0.05$). Specifically, the consumption of A2E by photooxidation was reduced by 93.8% in the case of quercetin and 38.8% by cyanidin-3-glucoside.

A longer irradiation period (3 min) and lower concentration of quercetin and cyanidin-3-glucoside was subsequently investigated (Fig. 3B). In the absence of antioxidant, only 2% A2E remained in the irradiated A2E compared with the non-irradiated A2E group. Importantly, addition of 100 μM quercetin completely inhibited the loss of A2E due to photooxidation. Cyanidin-3-glucoside also significantly ($p < 0.05$) inhibited A2E photooxidation at concentrations of 100 and 200 μM.

To evaluate the efficacy of quercetin and cyanidin-3-glucoside in inhibiting intracellular photooxidation of A2E, RPE cells were allowed to accumulate A2E after which the cells were incubated with the antioxidants. Irradiation of the cells at 430 nm led to A2E photooxidation as determined by quantifying cellular A2E levels by HPLC. The results obtained (Fig. 3C) were very similar to those obtained in cell-free assays (Fig. 3A and B), and indicated that quercetin and cyanidin-3-glucoside were able to inhibit A2E

photooxidation in RPE cells. Quercetin at the concentration of 50 μM almost completely inhibited A2E photooxidation in RPE cells.

3.4. Quercetin, cyanidin-3-glucoside and A2E-oxidation in a cell-free assay

We have reported that A2E undergoes photooxidation during irradiation with blue light, with formation of various oxygen-containing moieties (Ben-Shabat et al., 2002). Here, we investigated whether the protective effects of quercetin and cyanidin-3-glucoside were mediated, at least in part, by inhibiting A2E oxidation. A2E in DPBS was exposed to 430 nm irradiation followed by mass spectrometry (Fig. 4). The mass spectra of blue light-irradiated A2E disclosed a molecular ion peak at *m/z* 592, corresponding to the mass of A2E, and an additional series of higher molecular mass peaks (*m/z* 608, 624, 640, 656 and 688) representing the sequential insertion of oxygens at carbon-carbon double bonds. We have previously shown that these additional peaks correspond to A2E-oxidized species (Ben-Shabat et al., 2002). When A2E was irradiated in the presence of quercetin or cyanidin-3-glucoside (100 and 200 μM), the higher mass peaks (> *m/z* 592) were suppressed as evidenced by the overall reduction in peak intensity. Furthermore, quercetin appeared to be more effective than cyanidin-3-glucoside at reducing the generation of molecular ion peaks corresponding to oxidized-A2E since only two oxidized species were detectable (*m/z* 608 and 624) in the presence of quercetin as compared to three (*m/z* 608, 624 and 640) with cyanidin-3-glucoside.

3.5. The effect of quercetin and cyanidin-3-glucoside in inhibiting the reaction of photooxidized-A2E with GSH in a cell-free assay

We have previously shown that oxidized A2E can bind GSH (Yoon et al., 2011). To examine whether quercetin and cyanidin-3-glucoside inhibited the reaction between photooxo-A2E and GSH, we measured the levels of GSH in a cell-free assay. After GSH that had been incubated with photooxo-A2E produced by irradiating A2E, we observed a diminished availability of reduced GSH (Fig. 5). At the concentration of 200 μM, quercetin and cyanidin-3-glucoside completely protected GSH from reaction with photooxidized-A2E.

3.6. Quercetin and cyanidin-3-glucoside suppress MG-protein adduct formation in cell-free and cellular assays

To probe for evidence of the formation of protein-adducts and cross-linking by dicarbonyls released from photocleaved bisretinoid, we previously used RNase A as model since it is small and contains both lysine and arginine amino acid residues (Zhou et al., 2015). In those experiments, we monitored for cross-linking by SDS-PAGE. In the present experiments using competitive indirect ELISA, we tested for evidence that polyphenols inhibit the formation of MG-RNAse A adducts. After A2E and RNase A irradiation and incubation, MG-RNase A adducts were 2-fold more abundant than in the RNase A only sample (Fig. 6A and B). Quercetin and cyanidin-3-glucoside at a concentration of 500 μM significantly decreased the content of MG-RNase A adducts in this acellular assay ($p < 0.05$).

We also employed ARPE-19 cells to examine for MG-protein adducts. Here A2E-containing ARPE-19 cells were irradiated at 430 nm (Fig. 6C and D), the cells were lysed and the supernatants were assayed for MG-adducts. MG-BSA equivalent concentrations were

significantly higher in irradiated A2E-containing RPE cells as compared with untreated RPE ($p < 0.05$). Quercetin and cyanidin-3-glucoside (10 and 50 μM) markedly inhibited MG formation in the A2E-containing ARPE-19 cells that were irradiated at 430 nm ($p < 0.05$). Furthermore, the concentration of MG in the group of cyanidin-3-glucoside (50 μM) was 32.3% lower than that in quercetin (50 μM) group ($p < 0.05$).

3.7. Quercetin and cyanidin-3-glucoside suppress RAGE mRNA expression in cells irradiated to release dicarbonyls secondary to A2E photodegradation

Intracellular MG generated by A2E photoxidation and photodegradation has been shown to upregulate the expression of the cell surface receptor RAGE in RPE (Zhou et al., 2015). In the current experiments we found that 430 nm exposure of ARPE-19 cells that had accumulated A2E was associated with a 1.7-fold increase in RAGE mRNA expression ($p < 0.05$) (Fig. 7). At a concentration of 50 μM, quercetin and cyanidin-3-glucoside effectively reduced RAGE mRNA expression in the A2E-containing ARPE-19 cells that had been irradiated at 430 nm ($p < 0.05$).

3.8. Effect of quercetin and cyanidin-3-glucoside on HNE levels in rod OSs

Oxidation of polyunsaturated fatty acids generates complex mixtures of lipid peroxidation products such as malondialdehyde and HNE in the DHA-rich retina (Nowak, 2013). Since bisretinoids are photosensitizers that can initiate these reactions, we also assayed for the formation of HNE-BSA in rod OSs, incubated for 3 days with atRAL to generate bisretinoid production (Liu et al., 2000). HNE-BSA levels were significantly increased in the bisretinoid-burdened rod OSs after irradiation as compared to rod OSs incubated with atRAL without irradiation ($p < 0.05$) (Fig. 8). On the other hand, treatment with quercetin or cyanidin-3-glucoside (200 and 500 μM) before irradiation with 430 nm light, markedly decreased HNE-BSA levels in the atRAL-laden rod OSs irradiated at 430 nm ($p < 0.05$).

4. Discussion

Quercetin and cyanidin-3-glucoside with *ortho* hydroxyl group in the B ring exert stronger antioxidant activities due to the presence of two hydroxyl groups conferring antioxidant activity (RiceEvans et al., 1996; Wang et al., 2015). In keeping with this, we observed that quercetin and cyanidin-3-glucoside protected RPE cells against light damage by scavenging ROS and thereby inhibiting the A2E quenching of ROS that leads to the photooxidation and photodegradation of this intracellular bisretinoid. Quercetin and cyanidin-3-glucoside markedly inhibited the formation of MG-protein adducts and RAGE mRNA upregulation in response to carbonylation of RPE proteins. These antioxidants also suppressed the photooxidative processes in isolated OSs. Specifically, HNE-BSA levels were decreased in atRAL-laden rod OSs irradiated at 430 nm. The pathways impacted by the antioxidant activity of quercetin and cyanidin-3-glucoside in these experiments are summarized in Figure 9.

In a cell-free assay, quercetin and cyanidin-3-glucoside protected GSH from reaction with photooxidized-A2E and in doing so; it conserved levels of reduced GSH. In earlier work we found that GSH can donate hydrogen atoms to, and form conjugates with, photooxidized

forms of bisretinoids such as A2E; GSH can also react with its photocleavage products such as MG (Yoon et al., 2011). The adducts formed noncatalytically and by glutathione-S-transferase mediation. Based on these studies, we expect that the polyphenols quercetin and cyanidin-3-glucoside substituted for GSH as the hydrogen donor thus conserving GSH and converting the oxidized bisretinoid to non-toxic compounds.

While the experiments reported here employed *in vitro* models to examine mechanisms by which polyphenols can serve as antioxidants. The use of melanin-free ARPE-19 cells to study phototoxicity in these experiments avoided the biological variable that would be created by the use of human fetal RPE cultures having variable levels of light absorbing melanin. These studies are readily applicable to *in vivo* conditions. We have shown previously that bisretinoids can mediate retinal light damage. For instance, by measuring light-damage associated outer nuclear layer (ONL) thinning we demonstrated that mice carrying elevated levels of bisretinoid (*Abca4*$^{-/-}$ mice) undergo more pronounced photoreceptor cell damage than wild-type mice (Wu et al., 2014). In keeping with the age-related accumulation of bisretinoid, ONL thinning was also greater in 5-month versus 2-month-old mice. Conversely, in mice that exhibited no evidence of chromatographically detectable bisretinoid due to Rpe65 deficiency, light damage-triggered ONL thinning was not observed (Wu et al., 2014). Mice laden with augmented bisretinoid also exhibit accentuated carbonyl-adduct deposition in Bruch's membrane, excessive complement activation, Bruch's membrane thickening due to basal laminar deposits, and loss of photoreceptor cells (Kim et al., 2004; Maeda et al., 2009; Maeda et al., 2008; Radu et al., 2011; Weng et al., 1999; Zhou et al., 2015).

Oxidative mechanisms are viewed as being factors involved in AMD pathogenesis (Bian et al., 2012; Fritsche et al., 2013; Handa, 2012). For instance, the oxidant content of cigarette smoke may underlie the role of smoking in AMD risk (Handa, 2012). Moreover, several clinical and observation studies, including the Age-Related Eye Disease Study, have reported that dietary and supplementary intake of antioxidants, reduces the risk of AMD (Evans and Lawrenson, 2012; SanGiovanni et al., 2007; Sobrin and Seddon, 2014). Perhaps the beneficial effects of antioxidant intake are associated, to some extent, with inhibition of the photooxidative processes initiated by bisretinoids in the eye. Recent epidemiological studies (Cruickshanks et al., 1993; Fletcher et al., 2008; Fritsche et al., 2016; Klein et al., 2014; Tomany et al., 2004) and a meta-analysis (Sui et al., 2013) have pointed to a relationship between AMD and sunlight exposure.

Quercetin and cyanidin-3-glucoside, as abundant polyphenols in plant-based foods, are probably the most prominent dietary antioxidants. *In vivo* and *in vitro* studies have provided evidence that these compounds can protect RPE and photoreceptor cells from light and oxidative damage (Jang et al., 2005b; Saviranta et al., 2011; Wang et al., 2016; Wang et al., 2017). Quercetin defended human RPE cells from oxidative damage via suppression of pro-inflammatory cytokines and inhibition of apoptosis pathway (Cao et al., 2010). Among glucoside forms of four anthocyanins (cyanidin, delphinidin, malvidin, and pelargonidin), cyanidin-3-glucoside demonstrated the highest ROS inhibitory capacity in RPE cells (Wang et al., 2015). Here, we report that quercetin and cyanidin-3-glucoside protected RPE cells

against light damage *in vitro* by inhibiting the photooxidation and photodegradation of bisretinoid.

Acknowledgments

Supported by grants from the National Eye Institute EY12951 and P30EY019007 and a grant from Research to Prevent Blindness to the Department of Ophthalmology, Columbia University. The authors thank the China Scholarship Council for financial support of YW.

References

Anderson DH, Mullins RF, Hageman GS, Johnson LV. Perspective - A role for local inflammation in the formation of drusen in the aging eye. Am J Ophthalmol. 2002; 134(3):411–431. [PubMed: 12208254]

Ben-Shabat S, Itagaki Y, Jockusch S, Sparrow JR, Turro NJ, Nakanishi K. Formation of a nonaoxirane from A2E, a lipofuscin fluorophore related to macular degeneration, and evidence of singlet oxygen involvement. Angew Chem Int Edit. 2002; 41(5):814–817.

Bian Q, Gao S, Zhou J, Qin J, Taylor A, Johnson EJ, Tang G, Sparrow JR, Gierhart D, Shang F. Lutein and zeaxanthin supplementation reduces photooxidative damage and modulates the expression of inflammation-related genes in retinal pigment epithelial cells. Free Radical Bio Med. 2012; 53(6): 1298–1307. [PubMed: 22732187]

Cao X, Liu M, Tuo J, Shen D, Chan CC. The effects of quercetin in cultured human RPE cells under oxidative stress and in Ccl2/Cx3cr1 double deficient mice. Exp Eye Res. 2010; 91(1):15–25. [PubMed: 20361964]

Crabb JW, Miyagi M, Gu XR, Shadrach K, West KA, Sakaguchi H, Kamei M, Hasan A, Yan L, Rayborn ME, Salomon RG, Hollyfield JG. Drusen proteome analysis: An approach to the etiology of age-related macular degeneration. Proc Natl Acad Sci USA. 2002; 99(23):14682–14687. [PubMed: 12391305]

Cruickshanks KJ, Klein R, Klein BEK. Sunlight and age-related macular degeneration - the Beaver Dam Eye Study. Arch Ophthalmol. 1993; 111(4):514–518. [PubMed: 8470986]

Evans JR, Lawrenson JG. Antioxidant vitamin and mineral supplements for slowing the progression of age-related macular degeneration. Cochrane Database Syst Rev. 2012; 11:CD000254. [PubMed: 23152201]

Fletcher AE, Bentham GC, Agnew M, Young IS, Augood C, Chakravarthy U, de Jong P, Rahu M, Seland J, Soubrane G, Tomazzoli L, Topouzis F, Vingerling JR, Vioque J. Sunlight exposure, antioxidants, and age-related macular degeneration. Arch Ophthalmol. 2008; 126(10):1396–1403. [PubMed: 18852418]

Fritsche LG, Chen W, Schu M, Yaspan BL, Yu Y, Thorleifsson G, Zack DJ, Arakawa S, Cipriani V, Ripke S, Igo RP Jr, Buitendijk GHS, Sim X, Weeks DE, Guymer RH, Merriam JE, Francis PJ, Hannum G, Agarwal A, Armbrecht AM, Audo I, Aung T, Barile GR, Benchaboune M, Bird AC, Bishop PN, Branham KE, Brooks M, Brucker AJ, Cade WH, Cain MS, Campochiaroll PA, Chan CC, Cheng CY, Chew EY, Chin KA, Chowers I, Clayton DG, Cojocaru R, Conley YP, Cornes BK, Daly MJ, Dhillon B, Edwards A, Evangelou E, Fagemess J, Ferreyra HA, Friedman JS, Geirsdottir A, George RJ, Gieger C, Gupta N, Hagstrom SA, Harding SP, Haritoglou C, Heckenlively JR, Hoz FG, Hughes G, Ioannidis JPA, Ishibashi T, Joseph P, Jun G, Kamatani Y, Katsanis N, Keilhauer CN, Khan JC, Kim IK, Kiyohara Y, Klein BEK, Klein R, Kovach JL, Kozak I, Lee CJ, Lee KE, Lichtner P, Lotery AJ, Meitinger T, Mitchell P, Mohand-Saied S, Moore AT, Morgan DJ, Morrison MA, Myers CE, Naj AC, Nakamura Y, Okada Y, Orlin A, Ortube MC, Othman MI, Pappas C, Park KH, Pauer GJT, Peachey NS, Poch O, Priya RR, Reynolds R, Richardson AJ, Ripp R, Rudolph G, Ryu E, Sahel JA, Schaumberg DA, Scholl HPN, Schwartz SG, Scott WK, Shahid H, Sigurdsson H, Silvestri G, Sivakumaran TA, Smith RT, Sobrin L, Souied EH, Stambolian DE, Stefansson H, Sturgill-Short GM, Takahashi A, Tosakulwong N, Truitt BJ, Tsironi EE, Uitterlinden AG, van Duijn CM, Vijaya L, Vingerling JR, Vithana EN, Webster AR, Wichmann HE, Winkler TW, Wong TY, Wright AF, Zelenika D, Zhang M, Zhao L, Zhang K, Klein ML, Hageman GS, Lathrop GM, Stefansson K, Allikmets R, Baird PN, Gorin MB, Wang JJ, Klaver CCW, Seddon JM, Pericak-

Vance MA, Iyengar SK, Yates JRW, Swaroop A, Weber BHF, Kubo M, DeAngelis MM, Leveillard T, Thorsteinsdottir U, Haines JL, Farrer LA, Heid IM, Abecasis GR. Consortium AMDG. Seven new loci associated with age-related macular degeneration. Nat Genet. 2013; 45(4):433–439. [PubMed: 23455636]

Fritsche LG, Igl W, Bailey JNC, Grassmann F, Sengupta S, Bragg-Gresham JL, Burdon KP, Hebbring SJ, Wen C, Gorski M, Kim IK, Cho D, Zack D, Souied E, Scholl HPN, Bala E, Lee KE, Hunter DJ, Sardell RJ, Mitchell P, Merriam JE, Cipriani V, Hoffman JD, Schick T, Lechanteur YTE, Guymer RH, Johnson MP, Jiang Y, Stanton CM, Buitendijk GHS, Zhan X, Kwong AM, Boleda A, Brooks M, Gieser L, Ratnapriya R, Branham KE, Foerster JR, Heckenlively JR, Othman MI, Vote BJ, Liang HH, Souzeau E, McAllister IL, Isaacs T, Hall J, Lake S, Mackey DA, Constable IJ, Craig JE, Kitchner TE, Yang Z, Su Z, Luo H, Chen D, Hong O, Flagg K, Lin D, Mao G, Ferreyra H, Starke K, von Strachwitz CN, Wolf A, Brandl C, Rudolph G, Olden M, Morrison MA, Morgan DJ, Schu M, Ahn J, Silvestri G, Tsironi EE, Park KH, Farrer LA, Orlin A, Brucker A, Li M, Curcio CA, Mohand-Said S, Sahel JM, Audo I, Benchaboune M, Cree AJ, Rennie CA, Goverdhan SV, Grunin M, Hagbi-Levi S, Campochiaro P, Katsanis N, Holz FG, Blond F, Blanche H, Deleuze JF, Igo RP Jr, Truitt B, Peachey NS, Meuer SM, Myers CE, Moore EL, Klein R, Hauser MA, Postel EA, Courtenay MD, Schwartz SG, Kovach JL, Scott WK, Liew G, Tan AG, Gopinath B, Merriam JC, Smith RT, Khan JC, Shahid H, Moore AT, McGrath JA, Laux R, Brantley MA Jr, Agarwal A, Ersoy L, Caramoy A, Langmann T, Saksens NTM, de Jong EK, Hoyng CB, Cain MS, Richardson AJ, Martin TM, Blangero J, Weeks DE, Dhillon B, van Duijn CM, Doheny KF, Romm J, Klaver CCW, Hayward C, Gorin MB, Klein ML, Baird PN, den Hollander AI, Fauser S, Yates JRW, Allikmets R, Wang JJ, Schaumberg DA, Klein BEK, Hagstrom SA, Chowers I, Lotery AJ, Leveillard T, Zhang K, Brilliant MH, Hewitt AW, Swaroop A, Chew EY, Pericak-Vance MA, DeAngelis M, Stambolian D, Haines JL, Iyengar SK, Weber BHF, Abecasis GR, Heid IM. A large genome-wide association study of age-related macular degeneration highlights contributions of rare and common variants. Nat Genet. 2016; 48(2):134–143. [PubMed: 26691988]

Handa JT. How does the macula protect itself from oxidative stress? Mol Aspect Med. 2012; 33(4): 418–435.

Jang YP, Matsuda H, Itagaki Y, Nakanishi K, Sparrow JR. Characterization of peroxy-A2E and furan-A2E photooxidation products and detection in human and mouse retinal pigment epithelial cell lipofuscin. J Biol Chem. 2005a; 280(48):39732–39739. [PubMed: 16186115]

Jang YP, Zhou JL, Nakanishi K, Sparrow JR. Anthocyanins protect against A2E photooxidation and membrane permeabilization in retinal pigment epithelial cells. Photochem Photobiol. 2005b; 81(3):529–536. [PubMed: 15745429]

Kim SR, Fishkin N, Kong J, Nakanishi K, Allikmets R, Sparrow JR. Rpe65 Leu450Met variant is associated with reduced levels of the retinal pigment epithelium lipofuscin fluorophores A2E and iso-A2E. Proc Natl Acad Sci USA. 2004; 101(32):11668–11672. [PubMed: 15277666]

Kim SR, Jockusch S, Itagaki Y, Turro NJ, Sparrow JR. Mechanisms involved in A2E oxidation. Exp Eye Res. 2008; 86(6):975–982. [PubMed: 18439997]

Klein BEK, Howard KP, Iyengar SK, Sivakumaran TA, Meyers KJ, Cruickshanks KJ, Klein R. Sunlight exposure, pigmentation, and incident age-related macular degeneration. Invest Ophth Vis Sci. 2014; 55(9):5855–5861.

Liu JH, Itagaki Y, Ben-Shabat S, Nakanishi K, Sparrow JR. The biosynthesis of A2E, a fluorophore of aging retina, involves the formation of the precursor, A2-PE, in the photoreceptor outer segment membrane. J Biol Chem. 2000; 275(38):29354–29360. [PubMed: 10887199]

Maeda A, Golczak M, Maeda T, Palczewski K. Limited roles of Rdh8, Rdh12, and Abca4 in all-trans-retinal clearance in mouse retina. Invest Ophth Vis Sci. 2009; 50(11):5435–5443.

Maeda A, Maeda T, Golczak M, Palczewski K. Retinopathy in mice induced by disrupted all-trans-retinal clearance. J Biol Chem. 2008; 283(39):26684–26693. [PubMed: 18658157]

Mata NL, Weng J, Travis GH. Biosynthesis of a major lipofuscin fluorophore in mice and humans with ABCR-mediated retinal and macular degeneration. Proc Natl Acad Sci USA. 2000; 97(13):7154–7159. [PubMed: 10852960]

Milenkovic D, Jude B, Morand C. miRNA as molecular target of polyphenols underlying their biological effects. Free Radical Bio Med. 2013; 64:40–51. [PubMed: 23751562]

Nowak JZ. Oxidative stress, polyunsaturated fatty acids-derived oxidation products and bisretinoids as potential inducers of CNS diseases: focus on age-related macular degeneration. Pharmacol Rep. 2013; 65(2):288–304. [PubMed: 23744414]

Parish CA, Hashimoto M, Nakanishi K, Dillon J, Sparrow JR. Isolation and one-step preparation of A2E and iso-A2E, fluorophores from human retinal pigment epithelium. Proc Natl Acad Sci USA. 1998; 95(25):14609–14613. [PubMed: 9843937]

Radu RA, Hu J, Yuan Q, Welch DL, Makshanoff J, Lloyd M, McMullen S, Travis GH, Bok D. Complement system dysregulation and inflammation in the retinal pigment epithelium of a mouse model for stargardt macular degeneration. J Biol Chem. 2011; 286(21):18593–18601. [PubMed: 21464132]

RiceEvans CA, Miller NJ, Paganga G. Structure-antioxidant activity relationships of flavonoids and phenolic acids. Free Radical Bio Med. 1996; 20(7):933–956. [PubMed: 8743980]

SanGiovanni JP, Chew EY, Clemons TE, Ferris FL, Gensler G, Linblad AS, Milton RC, Seddon JM, Sperduto RD. Age-Related Eye Disease Study Research Group. The relationship of dietary carotenoid and vitamin A, E, and C intake with age-related macular degeneration in a case-control study - AREDS Report no. 22. Arch Ophthalmol. 2007; 125(9):1225–1232. [PubMed: 17846363]

Saviranta NMM, Veeroos L, Granlund LJ, Hassinen VH, Kaarniranta K, Karjalainen RO. Plant flavonol quercetin and isoflavone biochanin A differentially induce protection against oxidative stress and inflammation in ARPE-19 cells. Food Res Int. 2011; 44(1):109–113.

Sobrin L, Seddon JM. Nature and nurture- genes and environment- predict onset and progression of macular degeneration. Prog Retin Eye Res. 2014; 40:1–15. [PubMed: 24374240]

Sparrow JR, Fishkin N, Zhou JL, Cai BL, Jang YP, Krane S, Itagaki Y, Nakanishi K. A2E, a byproduct of the visual cycle. Vision Res. 2003a; 43(28):2983–2990. [PubMed: 14611934]

Sparrow JR, Gregory-Roberts E, Yamamoto K, Blonska A, Ghosh SK, Ueda K, Zhou J. The bisretinoids of retinal pigment epithelium. Prog Retin Eye Res. 2012; 31(2):121–135. [PubMed: 22209824]

Sparrow JR, Parish CA, Hashimoto M, Nakanishi K. A2E, a lipofuscin fluorophore, in human retinal pigmented epithelial cells in culture. Invest Ophth Vis Sci. 1999; 40(12):2988–2995.

Sparrow JR, Vollmer-Snarr HR, Zhou JL, Jang YP, Jockusch S, Itagaki Y, Nakanishi K. A2E-epoxides damage DNA in retinal pigment epithelial cells - Vitamin E and other antioxidants inhibit A2E-epoxide formation. J Biol Chem. 2003b; 278(20):18207–18213. [PubMed: 12646558]

Sparrow JR, Wu Y, Kim CY, Zhou J. Phospholipid meets all-trans-retinal: the making of RPE bisretinoids. J Lipid Res. 2010; 51(2):247–261. [PubMed: 19666736]

Sparrow JR, Zhou J, Ben-Shabat S, Vollmer H, Itagaki Y, Nakanishi K. Involvement of oxidative mechanisms in blue-light-induced damage to A2E-laden RPE. Invest Ophth Vis Sci. 2002; 43(4): 1222–1227.

Sui GY, Liu GC, Liu GY, Gao YY, Deng Y, Wang WY, Tong SH, Wang L. Is sunlight exposure a risk factor for age-related macular degeneration? A systematic review and meta-analysis. Brit J Ophthalmol. 2013; 97(4):389–394. [PubMed: 23143904]

Tomany SC, Cruickshanks KJ, Klein R, Klein BEK, Knudtson MD. Sunlight and the 10-year incidence of age-related maculopathy - The Beaver Dam eye study. Arch Ophthalmol. 2004; 122(5):750–757. [PubMed: 15136324]

Tremblay F, Waterhouse J, Nason J, Kalt W. Prophylactic neuroprotection by blueberry-enriched diet in a rat model of light-induced retinopathy. J Nutr Biochem. 2013; 24(4):647–655. [PubMed: 22832077]

Wang Y, Huo YZ, Zhao L, Lu F, Wang O, Yang X, Ji BP, Zhou F. Cyanidin-3-glucoside and its phenolic acid metabolites attenuate visible light-induced retinal degeneration in vivo via activation of Nrf2/HO-1 pathway and NF-B suppression. Mol Nutr Food Res. 2016; 60(7):1564–1577. [PubMed: 26991594]

Wang Y, Zhang D, Liu YX, Wang D, Liu J, Ji BP. The protective effects of berry-derived anthocyanins against visible light-induced damage in human retinal pigment epithelial cells. J Sci Food Agr. 2015; 95(5):936–944. [PubMed: 24909670]

Wang Y, Zhao L, Wang CT, Hu JM, Guo XX, Zhang D, Wu W, Zhou F, Ji BP. Protective effect of quercetin and chlorogenic acid, two polyphenols widely present in edible plant varieties, on visible light-induced retinal degeneration in vivo. J Funct Foods. 2017; 33:103–111.

Weng J, Mata NL, Azarian SM, Tzekov RT, Birch DG, Travis GH. Insights into the function of Rim protein in photoreceptors and etiology of Stargardt's disease from the phenotype in abcr knockout mice. Cell. 1999; 98(1):13–23. [PubMed: 10412977]

Wright JS, Johnson ER, DiLabio GA. Predicting the activity of phenolic antioxidants: Theoretical method, analysis of substituent effects, and application to major families of antioxidants. J Am Chem Soc. 2001; 123(6):1173–1183. [PubMed: 11456671]

Wu L, Ueda K, Nagasaki T, Sparrow JR. Light damage in Abca4 and Rpe65(rd12) mice. Invest Ophth Vis Sci. 2014; 55(3):1910–1918.

Wu Y, Yanase E, Feng X, Siegel MM, Sparrow JR. Structural characterization of bisretinoid A2E photocleavage products and implications for age-related macular degeneration. Proc Natl Acad Sci USA. 2010; 107(16):7275–7280. [PubMed: 20368460]

Yoon KD, Yamamoto K, Ueda K, Zhou JL, Sparrow JR. A novel source of methylglyoxal and glyoxal in retina: Implications for age-related macular degeneration. Plos One. 2012; 7(7):e41309. [PubMed: 22829938]

Yoon KD, Yamamoto K, Zhou JL, Sparrow JR. Photo-products of retinal pigment epithelial bisretinoids react with cellular thiols. Mol Vis. 2011; 17(201):1839–1849. [PubMed: 21850158]

Zhou JL, Ueda K, Zhao J, Sparrow JR. Correlations between photodegradation of bisretinoid constituents of retina and dicarbonyl adduct deposition. J Biol Chem. 2015; 290(45):27215–27227. [PubMed: 26400086]

Zhou JL, Cai BL, Jang YP, Pachydaki S, Schmidt AM, Sparrow JR. Mechanisms for the induction of HNE- MDA- and AGE-adducts, RAGE and VEGF in retinal pigment epithelial cells. Exp Eye Res. 2005; 80(4):567–580. [PubMed: 15781285]

Highlights

1. Quercetin and cyanidin-3-glucoside (C3G) reduced the consumption of A2E by photooxidation.
2. Quercetin and C3G inhibited the formation of photooxidized-A2E species.
3. Quercetin and C3G decreased the formation of methylglyoxal adducts in RPE.
4. Quercetin and C3G reduced the expression of mRNA encoding RAGE.

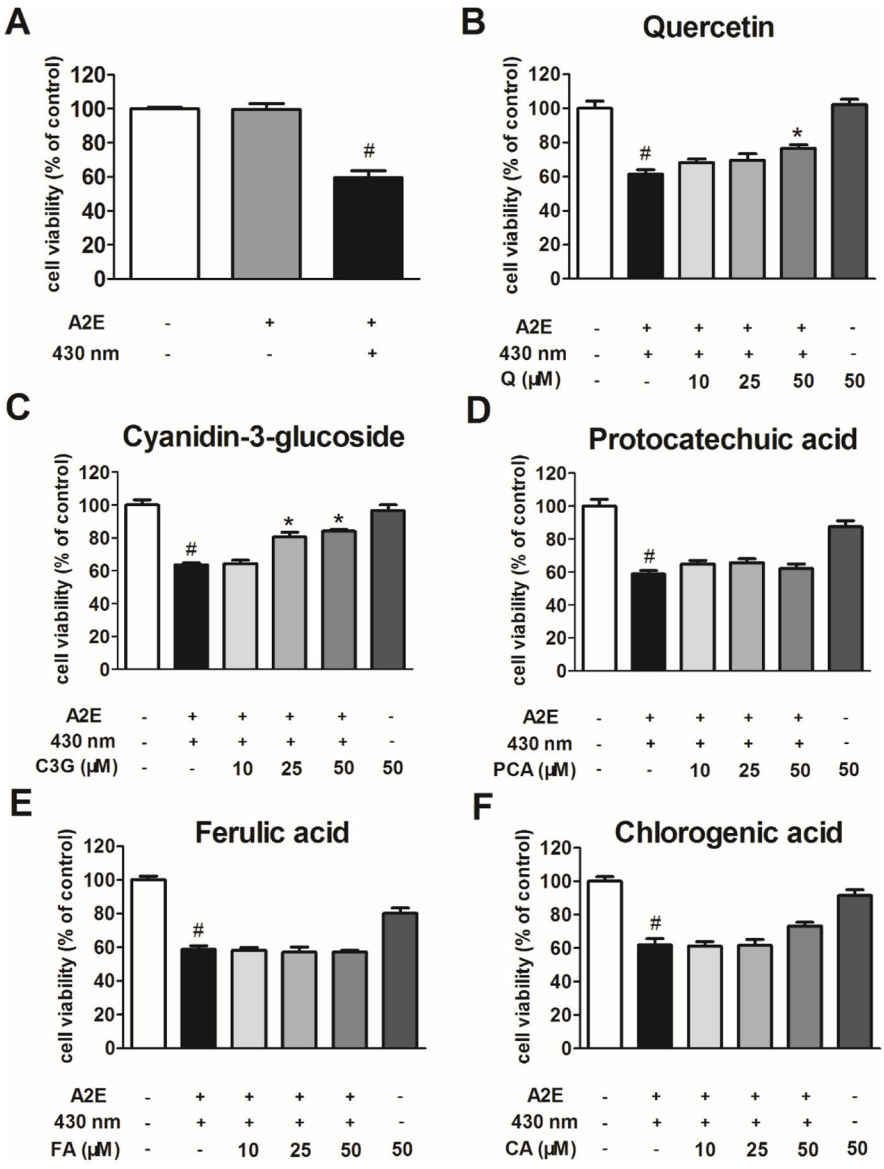

Figure 1.

Cell viability after 430 nm irradiation of ARPE-19 cells that have accumulated A2E. (A) A2E-laden RPE cells were exposed to 430 nm light for 20 min. After incubation for 18 hours, the cell viability was assayed by MTT assay. (B–F) Pre-treatment with quercetin (Q) and cyanidin-3-glucoside (C3G), protocatechuic acid (PCA), ferulic acid (FA), and chlorogenic acid (CA) (10, 25, and 50 μM) for 24 h before exposure to 430 nm light for 20 min. Only quercetin and cyanidin-3-glucoside attenuated blue light–related death of A2E-laden RPE. Mean ± S.E., 3 experiments. #, $p < 0.05$ as compared with untreated RPE cells; *, $p < 0.05$ as compared with A2E-containing irradiated RPE; one-way ANOVA and Tukey's multiple comparison test. +, treated; −, not treated.

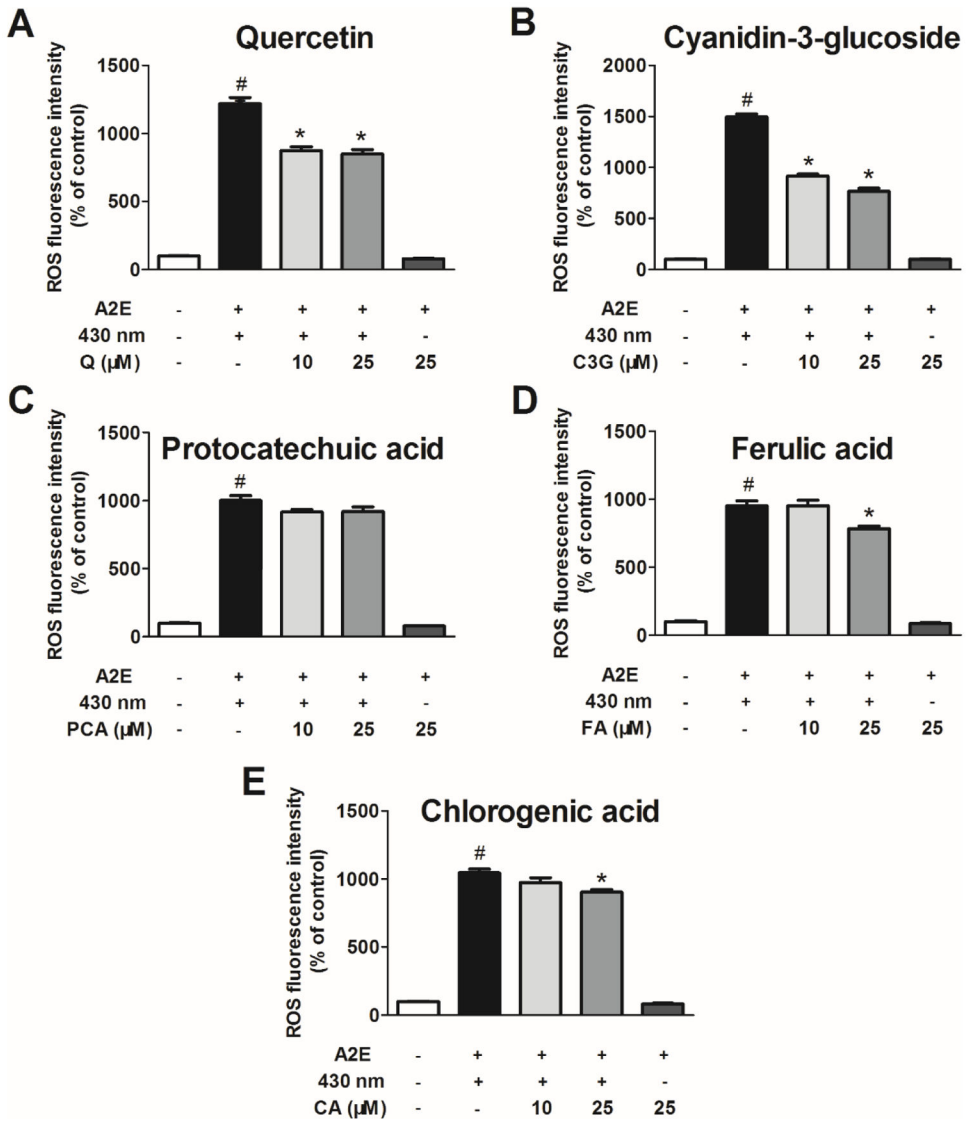

Figure 2.

Effects of quercetin (A), cyanidin-3-glucoside (B), protocatechuic acid (C), ferulic acid (D), and chlorogenic acid (E) on the generation of reactive oxygen species (ROS) in ARPE-19 cells that had accumulated A2E and were irradiated. The cells were treated with quercetin (Q), cyanidin-3-glucoside (C3G), protocatechuic acid (PCA), ferulic acid (FA), and chlorogenic acid (CA) 24 hours before irradiation at 430 nm for 30 min. Intracellular ROS levels were measured using 2′,7′-dichlorofluorescin diacetate (DCFH-DA). Mean ± S.E., 3 experiments. #, $p < 0.05$ as compared with untreated RPE cells; *, $p < 0.05$ as compared with A2E-containing irradiated RPE; one-way ANOVA and Tukey's multiple comparison test. +, treated; −, not treated.

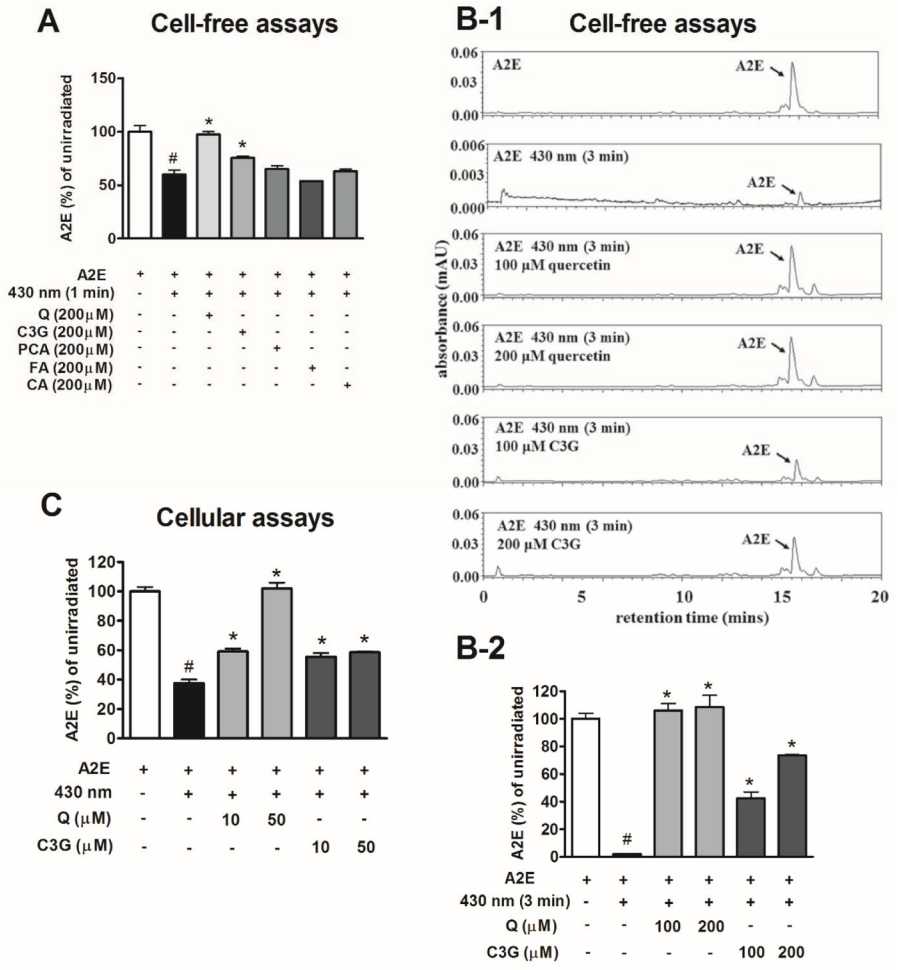

Figure 3.

The effect of antioxidants on A2E photooxidation in cell-free (A and B) and ARPE-19 cell-based assays (C). (A) A2E (100 μM) was photooxidized by 430 nm irradiation (1 min) in the presence and absence of quercetin (Q), cyanidin-3-glucoside (C3G), protocatechuic acid (PCA), ferulic acid (FA), and chlorogenic acid (CA) (200 μM) as indicated. The A2E content was quantified by HPLC using integrated peak intensities normalised to an external standard of A2E. The loss of A2E was diminished in the presence of quercetin and cyanidin-3-glucoside. (B) Reverse phase UPLC chromatogram demonstrating that A2E (100 μM) was photooxidized and consumed by 430 nm irradiation (3 min) as indicated by decreased peak area. A2E photooxidation was reduced in the presence of quercetin and cyanidin-3-glucoside (100 and 200 μM). (C) Quercetin and cyanidin-3-glucoside (10 and 50 μM 24 h) protect against blue light–induced A2E photo-oxidative degradation in ARPE-19 cells that had accumulated A2E (20 min irradiation). A2E in the cells was then quantified by UPLC. Mean ± S.E., 3 experiments. #, $p < 0.05$ as compared with A2E only (A and B) or A2E-containing cells that were not irradiated (C); *, $p < 0.05$ as compared with A2E and irradiation (A and B) or A2E-containing irradiated RPE (C); one-way ANOVA and Tukey's multiple comparison test. +, treated; −, not treated.

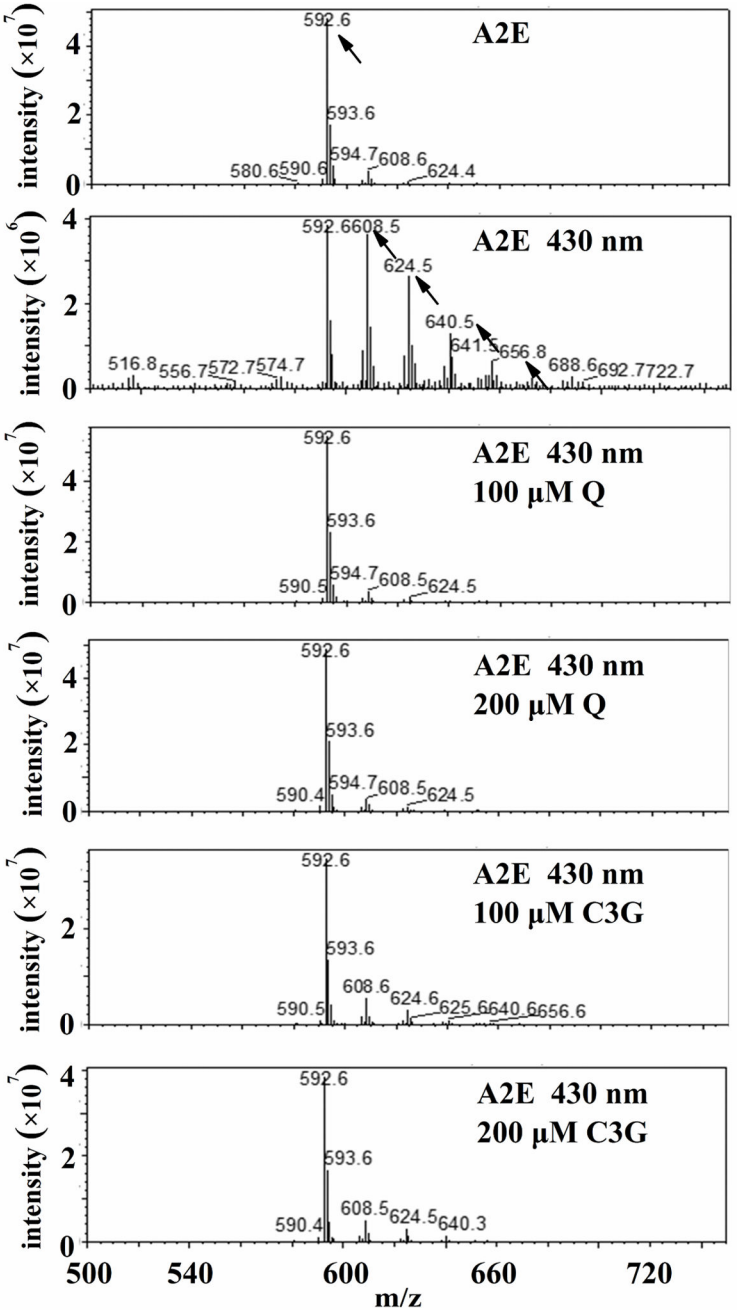

Figure 4.

Quercetin (Q) and cyanidin-3-glucoside (C3G) reduce the formation of oxidized-A2E. UPLC-MS of nonirradiated A2E (A2E control), A2E exposed to 430 nm light (A2E 430 nm light, 3 min), and A2E irradiated with blue light in the presence of quercetin (100 and 200 µM) or cyanidin-3-glucoside (100 and 200 µM) is shown. The molecular ion peak at m/z 592 corresponds to the molecular mass of A2E. The formation of ozidized-A2E by illumination is indicated by the presence of additional peaks that differ by mass 16. Illumination in the

presence of quercetin or cyanidin-3-glucoside reduces the formation of these oxidized species.

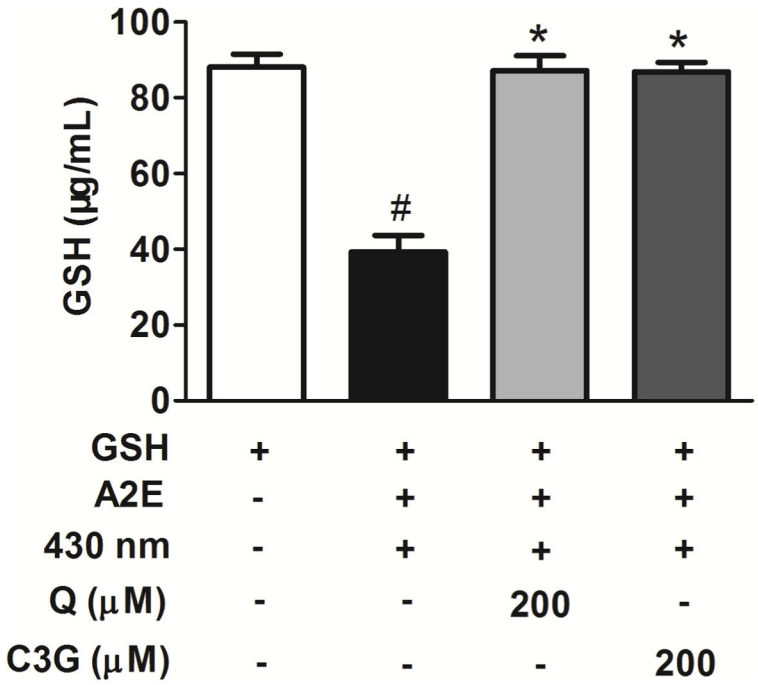

Figure 5.

Quercetin (Q) and cyanidin-3-glucoside (C3G) protect reduced glutathione (GSH) from reaction with photooxidized A2E. A2E was irradiated in the presence of GSH with or without quercetin and cyanidin-3-glucoside (200 μM), after which 5,5′-dithiobis-(2-nitrobenzoic acid (DTNB) was added to measure residual GSH. Mean ± S.E., 3 experiments. #, $p < 0.05$ as compared with no A2E and no irradiation; *, $p < 0.05$ as compared with A2E and irradiation; one-way ANOVA and Tukey's multiple comparison test. +, treated; −, not treated.

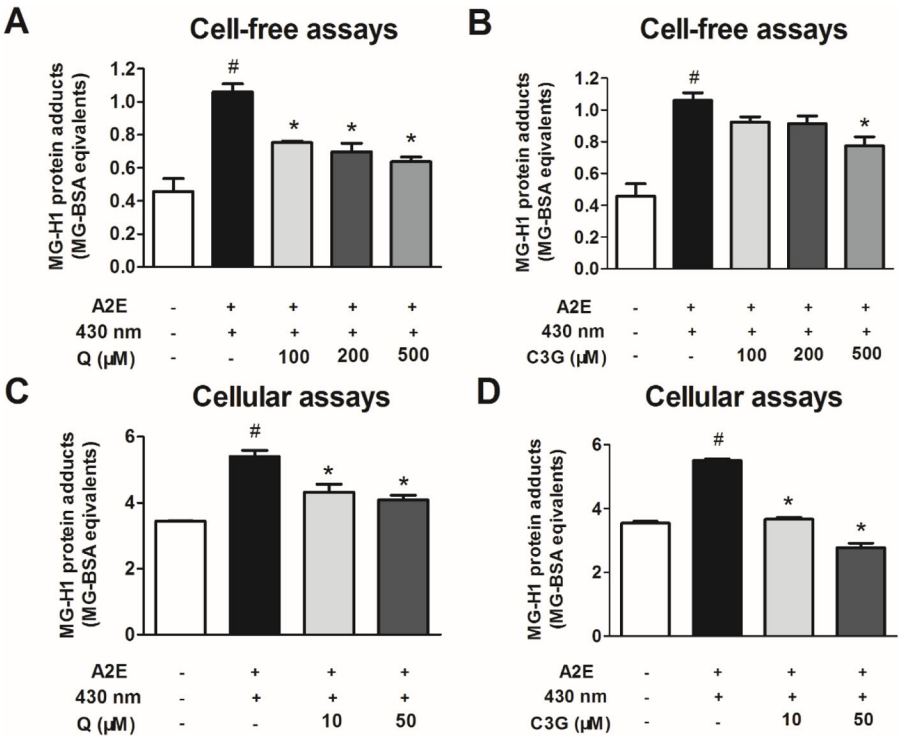

Figure 6.

Effect of quercetin (Q) and cyanidin-3-glucoside (C3G) (100, 200 and 500 μM) on methylglyoxal (MG)-RNase A-adducts in acellular assays (A and B). Measurement of MG-RNase A adducts 5 days after RNase A and A2E were irradiated at 430 nm for 30 min. Effect of quercetin and cyanidin-3-glucoside (10 and 50 μM) on MG-H1 protein adducts in lysates prepared from ARPE-19 cells that had accumulated A2E and were irradiated at 430 nm for 20 min (C and D). Mean ± S.E., 3 experiments. #, $p < 0.05$ as compared with RNase A only (A and B) or RPE only (C and D); *, $p < 0.05$ as compared with irradiated A2E and RNase A solution (A and B) or A2E-containing irradiated RPE (C and D); one-way ANOVA and Tukey's multiple comparison test. +, treated; −, not treated.

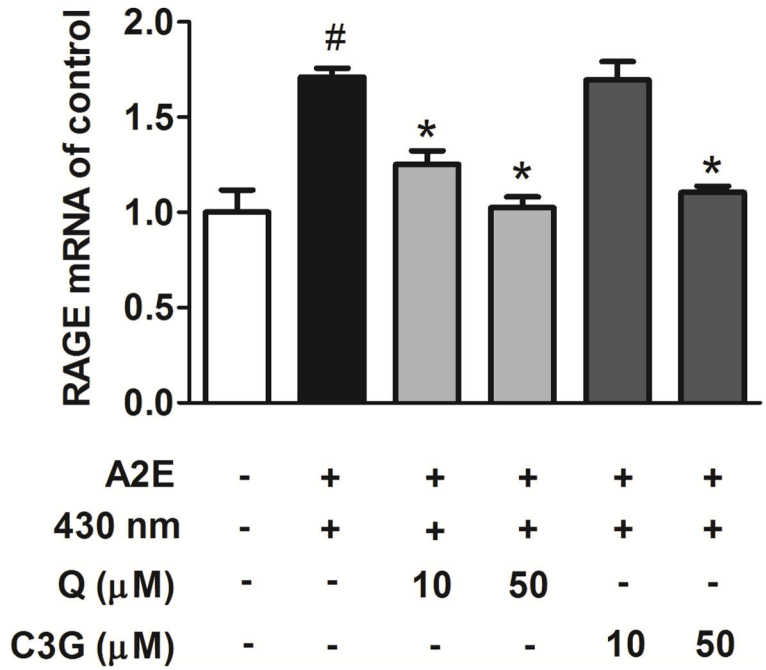

Figure 7.

Effect of quercetin (Q) and cyanidin-3-glucoside (C3G) (10 and 50 μM) on receptor for advanced glycation end products (RAGE) mRNA expression in ARPE-19 cells that had accumulated A2E and were irradiated at 430 nm for 20 min. RT-qPCR was performed with RNA purified from ARPE-19 cells. Mean ± S.E., 3 experiments. #, $p < 0.05$ as compared with RPE only; *, $p < 0.05$ as compared with A2E-containing irradiated RPE; one-way ANOVA and Tukey's multiple comparison test. +, treated; −, not treated.

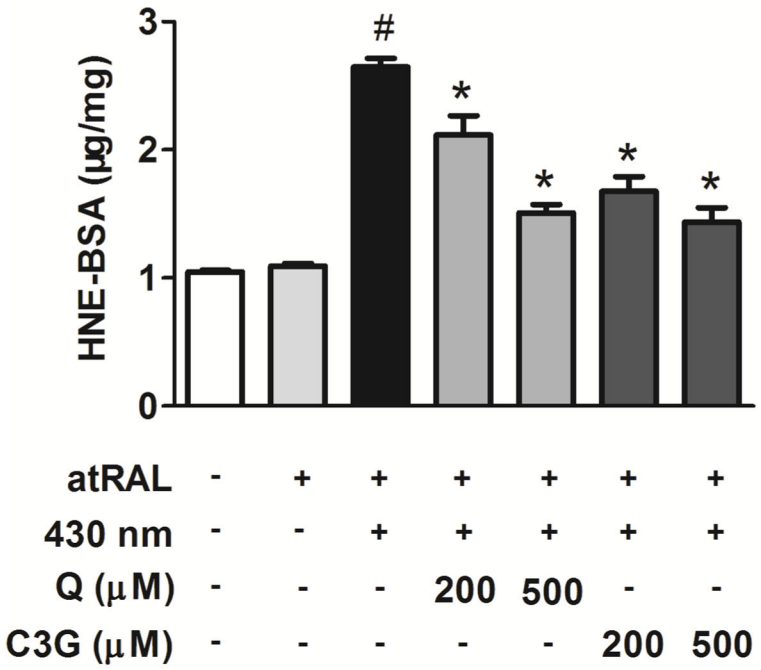

Figure 8.

Effect of quercetin (Q) and cyanidin-3-glucoside (C3G) on 4-hydroxynonenal (HNE) protein adducts in lysates prepared from bovine photoreceptor outer segments that were incubated with all *trans*-retinal (atRAL) and irradiated at 430 nm for 30 min. Mean ± S.E., 3 experiments. #, $p < 0.05$ as compared with rod outer segment only; *, $p < 0.05$ as compared with all *trans*-retinal accumulated and irradiated rod outer segment; one-way ANOVA and Tukey's multiple comparison test. +, treated; −, not treated.

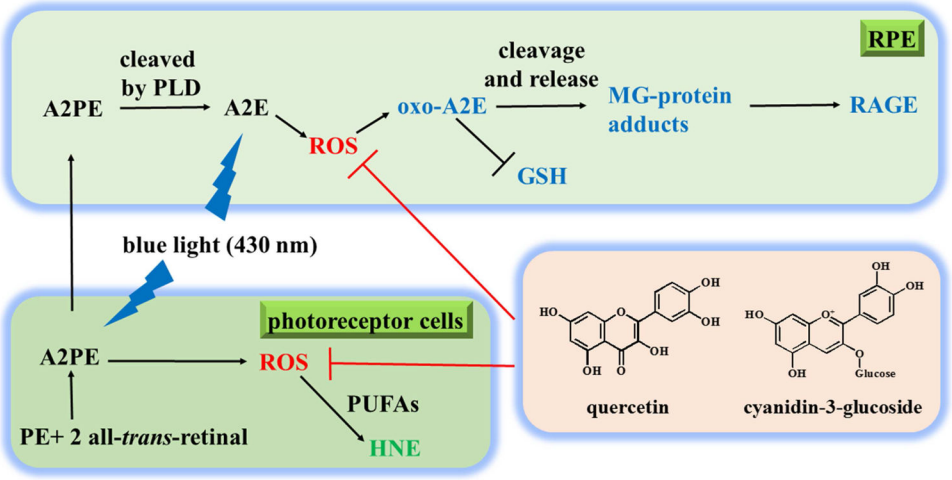

Figure 9.

Mechanisms by which quercetin and cyanidin-3-glucoside may afford protection. Quercetin and cyanidin-3-glucoside scavenge reactive oxygen species (ROS), thus decreasing formation of photooxo-A2E (oxo-A2E), reducing release of methylglyoxal (MG) and protecting against the upregulation of receptor for advanced glycation end-products (RAGE) in retinal pigment epithelial (RPE) cells. Quercetin and cyanidin-3-glucoside also inhibited 4-hydroxynonenal (HNE)-protein adduct formation in photoreceptor outer segments. Bisretinoid photoreactive species (e.g. A2PE) that form in outer segments due to reactions of all-trans-retinal with phosphatidylethanolamine (PE) can generate ROS thereby causing the peroxidation of polyunsaturated fatty acids (PUFAs) and leading to release of HNE that modifies proteins.